

## TIDAL ASYMMETRY AND ESTUARINE MORPHOLOGY

J. DRONKERS

Division of Tidal Waters, Rijkswaterstaat, v. Alkemadeaan 400, 2597 AT The Hague, The Netherlands

### ABSTRACT

Estuarine morphology is to a large extent determined by the residual sediment transport pattern. However, the inverse statement is also true. Residual sediment transport depends on differences in magnitude and duration between ebb and flood tidal currents. Such differences ("tidal asymmetry") are produced by the distortion of the tidal wave propagating on the coastal shelf and entering bays and estuaries. In this study the relationship between tidal asymmetry and estuarine morphology is investigated. Based on theoretical considerations some general principles are derived and compared with field observations.

### 1. INTRODUCTION

The evolution of an estuary depends essentially on two processes:

- the long-term averaged sediment supply from inland or coastal origin, and the direction and magnitude of the long-term averaged sediment transport,

- abrupt changes in the estuarine morphology caused by storm surges or by engineering works.

The present study is concerned with the first process. The second process will be invoked when some practical examples are discussed.

It is often conjectured that estuaries tend to fill in with sediment and will, therefore, ultimately disappear. In the final stage of evolution, river water is discharged directly on the coastal shelf (SCHUBEL & MEADE, 1977). However, temporarily certain estuaries may behave as erosion basins, as a consequence of externally induced changes in sediment supply or flow regime. Whether stable estuaries exist (sediment inflow on the average balanced by sediment outflow) is not known, and it also seems an academic question: there always exist external con-

ditions (e.g. the mean sea level) subject to variations (POSTMA, 1980).

The sediment supply and sediment transport pattern in an estuary depend on several factors, some of which will be discussed in more detail:

- (a) The river inflow, with related to it (a1) an input of sediment and (a2) a cross-sectional flow structure affected by density differences. Density differences tend to increase flood currents in the deepest parts of the channel, in particular in the lower half of the vertical, and tend to decrease flood currents near the surface and in the shallow parts of the cross-section. The inverse holds for the ebb currents.

This flow structure has an important impact on the sediment transport. It has been discussed already by many authors, for example POSTMA (1967), FESTA & HANSEN (1978), ODD & OWEN (1972), ALLEN *et al.* (1977), ARIATHURAI *et al.* (1977). The present study will not enter further into details.

- (b) The sediment characteristics. In general a wide spectrum of sediment types is present in suspension at the same time. In this study only a crude distinction between "fine" and "coarse" sediment will be made, based mainly on fall velocity  $w$  (for "coarse" sediment  $w \geq 10^{-1} \text{ m}\cdot\text{s}^{-1}$ , for fine sediment  $w \leq 10^{-2} \text{ m}\cdot\text{s}^{-1}$ , see also section 2). For both sediment types two transport modes exist: along the bottom (coarse grains moving by traction in the bedload, fine sediment moving as fluid mud), or as suspended load. As will be argued in section 2, tidal asymmetry affects suspension transport in particular. The influence of tidal asymmetry on the residual fluxes of coarse and fine sediment is different, owing to different transport properties: the suspension load of coarse sediment is strongly limited by the current speed and it adapts to changes in the current speed rapidly in comparison with the tidal time scale. For fine sediment, saturation of the suspended load seldom occurs. Most fine sediment settles only at very low current speed and the settling time delay is important.

-(c) Wind waves, swell. The purely wave-induced sediment transport is relatively less important in estuaries than on the coastal shelf. However, the influence of wind waves, in tidal flat areas at high water, on the resuspension of sediment is a significant phenomenon (ANDERSON, 1972; McDOWELL & O'CONNOR, 1977). In combination with subsequent tidal transport, it can cause a substantial seaward sediment flux.

-(d) The current velocity distribution and in particular its variation during a tidal cycle. Two elements are mainly responsible for residual sediment fluxes (in addition to density influences):

-(d1) The tidal variation at the sea entrance, which bears the characteristics of tidal wave propagation on the coastal shelf (amplification, distortion),

-(d2) The tidal propagation inside the tidal basin, generally consisting of a complex geometrical system formed by meandering and braiding channels and tidal flats.

The present study is mainly devoted to aspect (d): the analysis of tidal wave deformation in shallow systems with a regular or a complex geometry, and its impact on the residual sediment flux. Globally speaking the following features of tidal wave deformation are relevant for residual sediment transport (a more detailed discussion is presented in section 2):

- a difference between the maximum tidal currents during ebb and flood, which in particular affects the residual flux of the coarse suspended fraction,

- a difference between the slack water periods preceding ebb and flood, which particularly influences the residual flux of the fine suspended fraction.

In sections 3 and 4 it will be shown that a tidal wave changes its original sinusoidal shape and becomes asymmetric when it enters a tidal basin:

- if the mean water depth is so small that the tidal variation cannot be neglected; the geometry changes significantly with tidal level, or

- if the velocity field changes significantly over a distance comparable with the tidal excursion (for example, the channel geometry varies over such distances).

In addition, the sinusoidal shape of a tidal wave is altered by the quadratic dependence of bottom friction on the current speed. However, this quadratic character conserves the ebb-flood symmetry, and no residual sediment flux results. Also, the main characteristics of tidal distortion will be demonstrated on a simplified model with bottom friction depending linearly on the current velocity. In the appendix, first order approximations of the tidal wave deformation due to different non linear terms are presented for a

uniform rectangular basin with and without wave reflection.

Section 2 deals with the influence of tidal asymmetry on the residual sediment flux. In sections 3 and 4, the propagation and distortion of a tidal wave in different types of basins is discussed: tidal rivers with no substantial wave reflection (section 3) and almost co-oscillating short tidal basins with a complex geometry (section 4). In section 5 field observations of the residual sediment flux in two tidal basins in the Netherlands are discussed as an example. In section 6 the principal results are briefly summarized.

Many of the ideas today forming the foundation of the geomorphological science of estuarine and coastal environments have been developed by Henk Postma. His scientific work has been an important source of inspiration for this study.

Acknowledgements.—Numerical model simulations were performed by M. Geurtz in order to check the general validity of several statements on the relationship between tidal asymmetry and estuarine morphology. Improvements of the draft have been suggested by J.R. van der Berg, L. Kohsiek and C. Louisse. The figures were prepared by Th. Vogel and the typewriting by Mrs E. Goldbach.

## 2. SEDIMENT TRANSPORT DUE TO TIDAL ASYMMETRY

This section contains some general considerations on the residual flux of sediment in tidal environments. Successively, bed load transport and suspension transport will be discussed for both coarse and fine sediment.

Bed load transport of coarse sediment consists of grains with a diameter in the order of 200  $\mu\text{m}$  or larger, rolling or jumping over the bed (YALIN, 1972; McDOWELL & O'CONNOR, 1977; HEATHERSHAW, 1981). The velocity of such grains is much smaller than the current speed. As a consequence the local dominance of ebb or flood currents mainly determines the residual bed load flux. A general feature of sandy bays and estuaries is the presence of a pattern of alternating ebb and flood channels (VAN VEEN, 1950; ROBINSON, 1960). As stated by LAMBIASE (1980), slow-moving grains transported by traction are trapped in such channel systems. (On the contrary, suspended grains generally move fast enough to bypass channel sections where locally the residual current is opposed). The conclusion is that in most sandy estuaries an ebb-flood asymmetry of the tidal wave does not greatly affect the residual flux of bed load sediment.

Transport of fine sediment along the bottom is ge-

nerally described as "fluid mud". This phenomenon has been observed in several estuaries (e.g. the Thames and the Gironde) and is associated with the occurrence of a turbidity maximum (INGLIS & ALLEN, 1957; ALLEN *et al.*, 1977). In these estuaries a distinct ebb-flood asymmetry in the near-bottom layer is caused by estuarine gravitational circulation. Again, an additional ebb-flood asymmetry due to tidal wave distortion is not the major factor for residual transport, although it may have a quantitatively significant influence.

Suspension transport of coarse sediment possesses the following characteristics: the maximum sediment load in suspension at a given current speed is limited and depends on particle size and density (BRUUN, 1978; DYER, 1980). The saturation load is rapidly reached (as compared to the tidal time scale). Commonly found sediment particles with these transport characteristics in the estuarine environment are fine sands (size on the order of 100  $\mu\text{m}$ ) and large biologically bound aggregates (size on the order of a few hundred  $\mu\text{m}$ ) (BIGGS, 1978; POSTMA, 1980; EISMA *et al.*, 1980). The saturation load increases very strongly with increasing current velocity. Therefore, a tidal asymmetry in the current velocity variation may affect the residual transport of coarse sediment. The most significant asymmetry in this respect is a difference between the maximum current velocities occurring during flood and ebb. For example, if flood velocities exceed ebb velocities in compensation of a longer ebb duration, then a residual landward transport of coarse sediment will exist.

In many estuaries, the suspended load is mainly composed of fine sediment: particles with a size between 1 and 10  $\mu\text{m}$  (quartz, feldspar, clay minerals) and aggregates with a size up to 100  $\mu\text{m}$  (MEADE, 1972; EISMA *et al.*, 1980). The transport of this material is more complicated than the transport of coarse sediment. This is due in particular to the cohesive properties (consolidation and flocculation) and related time lag effects. Even at rather small current velocities (a few  $\text{dm}\cdot\text{s}^{-1}$ ), an important load of fine sediment can be maintained in suspension. Actually, saturation seldom occurs. The concentration of fine suspended sediment is limited by the availability of erodible bottom material, *i.e.* by consolidation or by the presence of an overlying coarse sediment layer. Weakly consolidated fine sediment is resuspended when the current velocity reaches a critical value  $u_e$  (see, for example, CREUTZBERG & POSTMA, 1979; MEHTA & PARTHENIADES, 1982; DRONKERS, 1985). When the current velocity increases further, more consolidated fine sediment and deeper layers may be brought in suspension.

Part of the fine sediment load settles in the period around slack water, in particular the aggregates with a size on the order of 100  $\mu\text{m}$  and larger (POSTMA, 1960; CHASE, 1980). Adhesion on the bottom may occur when the current speed has dropped below a threshold value  $u_d$ ,  $u_d < u_e$  (EINSTEIN & KRONE, 1962). It follows that the fine sediment load responds more strongly to tidal variations in the period around slack water than around maximum current speed. The slack water periods will be designated as SBE and SBF: Slack tide Before Ebb (seaward flow) and Slack tide Before Flood (landward flow), respectively.

For the residual transport of fine suspended sediment, an approximate analytical expression has been derived by DRONKERS (1985), based on a qualitative description by POSTMA (1961). In this derivation the excursion of sediment particles through the estuary is followed during a tidal cycle. Relevant quantities are the water depth and the current velocity variation, which are compared at  $t^+$  (=SBE) at a location  $x^+$  (=the landward limit of the tidal excursion), and at  $t^-$  (=SBF) at a location  $x^-$  (=the seaward limit). The resulting expression for the net transported sediment mass through a cross section  $x = 1/2(x^+ + x^-)$  during a tidal cycle reads:

$$M = \mu^+ \lambda^+ - \mu^- \lambda^- \quad (1)$$

where  $\mu^+$  (respectively  $\mu^-$ ) is the amount of sediment settled on the bottom at  $x^+$  (respectively  $x^-$ ) in the period of SBE (respectively SBF), and  $\lambda^+$  (respectively  $\lambda^-$ ) is the distance travelled by fluid parcels in the SBE (respectively SBF) time interval  $\Delta t^+$  (respectively  $\Delta t^-$ ) during which the fine fraction remains settled. The quantities  $\mu^\pm$  and  $\lambda^\pm$  can be evaluated from the approximate expressions:

$$\mu^\pm(x) = \omega^\pm(x) \cdot \text{max. susp. conc.}(x)$$

$$\omega^\pm(x) = A_s(x^\pm, t^\pm) \left[ 1 - \exp\left(-w \frac{\Delta t_d^\pm(x^\pm)}{h(x^\pm, t^\pm)}\right) \right] \quad (2)$$

$w$  = fall velocity,  $A_s$  = stream cross-section,  $\Delta t_d$  = time interval for which  $|u| < u_d$ ,

$$\lambda^\pm(x) = 1/2 u_e \cdot \Delta t^\pm(x^\pm) \quad (3)$$

The physics behind these equations is obvious: the amount of sediment  $\mu^+$ , which is settled per unit length in the period around SBE, will not follow the tidal motion before the ebb current reaches the critical speed for erosion  $u_e$ . In this lapse of time the

settled sediment is displaced with respect to the suspended sediment in landward direction over a distance which on the average equals  $\lambda^+$ . Around SBF a similar relative displacement will occur of a sediment mass  $\mu^-$  in seaward direction over an average distance  $\lambda^-$ .

The equations (2) and (3) show that a landward residual flux of fine sediment is favoured if:

- the channel depth decreases in landward direction,  $h(x^+, t^+) < h(x^-, t^-)$ ,
- the velocity variation is slower around SBE than around SBF,

$$| du/dt |_{x^+, t^+} < | du/dt |_{x^-, t^-}$$

This last condition can be realized either by a distortion of the tidal wave (see the sections 3 and 4) or by a landward decrease of the current velocity. The latter aspect has been demonstrated in particular by VAN STRAATEN & KUENEN (1959).

Finally the influence of wind waves should be mentioned. In addition to tidal currents, short waves also contribute to bringing and keeping sediment in suspension. Wave energy dissipation is mainly restricted to shallow regions, with water depth in the order of a few meters or less. In estuaries with landward decreasing depth, the amount of sediment deposited in the period around SBE is more strongly decreased by wave action than the amount deposited around SBF. In such estuaries wind waves counteract a landward residual transport of fine sediment by tidal currents, or enhance a seaward residual transport.

The seaward flux due to wind waves can be particularly important in estuaries with high tidal flats (situated above mean sea level). In a meandering channel system such high tidal flats are built up by a near-bottom flow component which is directed up slope at the headlands during both ebb and flood (HEATHERSHAW & HAMMOND, 1980). The fine sediment eroded from the tidal flats by waves in the period around high water remains in suspension during most of the ebb period and is, therefore, transported a long distance in seaward direction. Coarse sediment is also brought in suspension by wind waves. It will be deposited sooner than the fine sediment and will thus be transported less far by the ebb current. However, this coarse sediment is not so easily resuspended by the flood current; in tidal flat estuaries wind waves also cause a net seaward transport of coarse sediment. In other words: tidal flat formation by tidal currents, counteracted by wind waves may finally lead to an export of sediment.

### 3. DISTORTION OF A NON-REFLECTED TIDAL WAVE

The cross-sectionally integrated tidal equations, valid for wide shallow basins ( $b \gg h$ ), read:

$$\frac{d\xi}{dt} + \frac{1}{b} \frac{d}{dx} (A_s u) = 0 \quad (4)$$

$$\frac{du}{dt} + u \frac{du}{dx} + g \frac{d\xi}{dx} + F \frac{u}{h + \xi} = 0 \quad (5)$$

Here the total cross-section  $A$  (width at the water surface =  $b$ ) has been divided into two parts. The entire transport takes place in one part (cross section =  $A_s$ , average depth =  $h$ ). The other part (which is shallow, the depth averaged velocity being less than, about,  $0.3 u$ ) is considered to act as a storage area only. The friction term is not quadratic but linear with the current velocity. As explained, essentially this simplification does not affect the ebb-flood asymmetry of the tidal wave. Typical values of the friction coefficient  $F$  range between  $10^{-3}$  and  $5 \cdot 10^{-3} \text{ m} \cdot \text{s}^{-1}$ .

In this section long inshore tidal basins or tidal rivers are considered in which the tidal wave can propagate without substantial reflection. In practice, this implies a geometry without important cross-sectional variations. If a sufficiently regular geometry is assumed, the equations (1) and (2) can be simplified to the equations (A1) and (A2) of the appendix. In these equations three non-linear terms are responsible for the distortion of the tidal wave. The influence of these terms is demonstrated in the appendix and the Figs 10a to c. A qualitative discussion is presented below.

In the continuity equation (A1) the term  $\xi du/dx$  represents the tidal variation of water depth. On the average the water depth is larger during flood than during ebb. Therefore, a residual discharge in the wave propagation direction will exist unless the flood currents are smaller than the ebb currents. This phenomenon is usually described as "Stokes drift".

In the momentum equation (A2) the term  $u du/dx$  constitutes a contribution to the acceleration  $du/dt$ , which tends to increase the magnitude of the acceleration during flood and to decrease the magnitude during ebb. The result is contrary to the Stokes drift: a relatively shorter flood period with relatively higher velocities, as compared to the ebb period. However, Stokes drift is the dominating effect, see Fig. 10a.

A very important aspect of the non-linear terms  $u d\xi/dx$  and  $u du/dx$  is to introduce total time derivatives  $d/dt$  instead of partial derivatives  $\partial/\partial t$ ,  $d/dt = \partial/\partial t + u \partial/\partial x$ . For an observer moving with the

current velocity  $u$  the tidal equations remain linear (except for the term  $\xi du/dx$ ). As a consequence, the wave crest and wave trough propagate at different velocities,  $c + u_{max}$  and  $c - u_{max}$  respectively. Here  $c = \sqrt{gh}$  and  $u_{max} = ac/h$ . The term  $\xi du/dx$  yields a larger water depth for wave propagation in the crest than in the trough  $\sqrt{g(h+a)}$  and  $\sqrt{g(h-a)}$  respectively. Combining both effects the wave crest moves approximately with velocity  $\sqrt{gh} (1 + \frac{3a}{2h})$  and the trough with velocity  $\sqrt{gh} (1 - \frac{3a}{2h})$ . As a result, the rising part of the wave surface becomes steadily steeper, and the falling part steadily flatter, see Fig. 10a. This result was established long ago by AIRY (1842). Ultimately this deformation leads to a tidal bore and wave breaking.

A tidal bore develops in an estuary if the tidal range  $\Delta\xi$  is sufficiently large and if the bottom slope  $I_b$  in the zone situated around mean coastal sea level is sufficiently gentle (COMOY, 1881; LYNCH, 1982)

$$\Delta\xi \geq \frac{1}{\pi} I_b \cdot T \cdot \sqrt{g(h + \langle \xi \rangle)}$$

See Fig. 1a. Well-known examples are the rivers Tsientang, Severn and Hooghly.

In most tidal rivers this final stage of distortion is not reached. In general only a slightly steeper rise than decrease of water levels is observed. Accordingly, the slack water period preceding flood is longer than the slack water period preceding ebb. Examples are shown in Fig. 2. As discussed in section 2, import of fine sediment is favoured by this tidal asymmetry over export.

From the analysis of IWAGAKI & SAKAI (1974) it follows that the above discussion of wave deformation

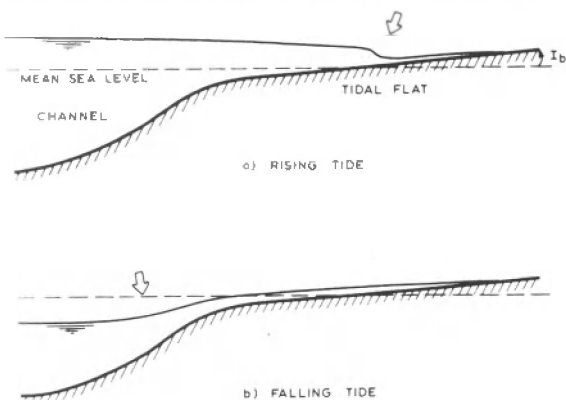


Fig. 1. Tidal propagation on a gently sloping tidal flat. a. Formation of a bore during rising tide. b. Development of a strong surface inclination during ebb.

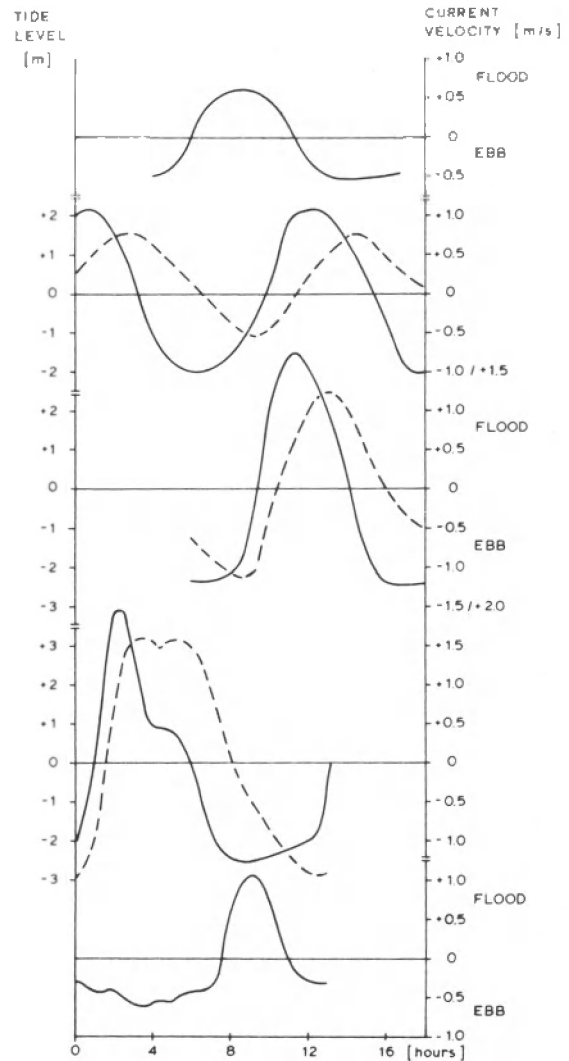


Fig. 2. Field observations of tidal wave propagation in rivers.

by non-linear terms remains qualitatively valid if, instead of a constant depth, a slowly decreasing depth in the wave propagation direction is considered, which is in general more realistic for tidal rivers.

A particular aspect of the previous discussion is the tidal wave distortion in shallow coastal seas. Along the western coast of the Netherlands a semidiurnal tidal wave propagates from south to north, belonging to the amphidromic system in the Southern Bight of the North Sea. Along the northern coast of the Netherlands a semidiurnal tidal wave propagates from west to east, belonging to the amphidromic system of the central North Sea. Both tidal waves are distorted when running along the Dutch coast, and on the way exhibit an increasingly stronger rise and slower

fall, see Fig. 3. This has important consequences for the asymmetry of the co-oscillating tides in the Dutch tidal basins and estuaries, as will be shown in sections 4 and 5. The generation of higher harmonic tidal constituents in coastal shelf seas and their influence on sediment transport have also been discussed recently by PINGREE *et al.* (1984).

So far friction has been neglected. However, frictional influences cannot be ignored in most coastal seas and estuaries. The non-linearity of the friction term causes, in the uniform systems considered here, a larger frictional influence at low water than at high water, yielding (slightly) larger flood than ebb velocities (see Fig. 10b). Another aspect is the retardation of the tidal velocity with respect to the water level elevation. The maximum flood velocity occurs during rising tide, the maximum ebb velocity during falling tide; the magnitude depends on the actual inclination of the water surface. The formerly discussed steeper rise of the tide and slower decrease caused by the non-linear terms  $u \partial u / \partial x$  and  $\partial u \xi / \partial x$  produce, in combination with friction, a relatively larger flood velocity and a relatively smaller ebb velocity. These effects counteract and even dominate the Stokes drift, as shown in Fig. 10c. The occurrence of larger maxi-

mum flood velocities than ebb velocities is a commonly observed feature in tidal rivers (at least at low river runoff), see Fig. 2. It tends to favour landward transport of sediment over seaward transport.

As mentioned in section 1, river runoff produces a cross-sectional distribution of current velocities which enhances seaward transport in the near surface part, but counteracts seaward transport in the deeper parts of the channel. This phenomenon will not be discussed here, but should be considered for practical applications. Finally, it is noted that river runoff not only influences the cross-sectional distribution of currents. A distortion of the tidal wave may also result, at least if river and tidal discharges are comparable (GODIN, 1985). The main cause is the quadratic dependence of bottom shear stress on current speed (HEATH, 1981). However, the direction of the residual sediment transport is not strongly influenced: at high river runoff seaward transport dominates (MIGNIOT, 1968).

#### 4. DISTORTION OF A STANDING TIDAL WAVE

In basins with a length  $l$  much shorter than the tidal wavelength  $L$  or a constriction at a distance  $l$  from the

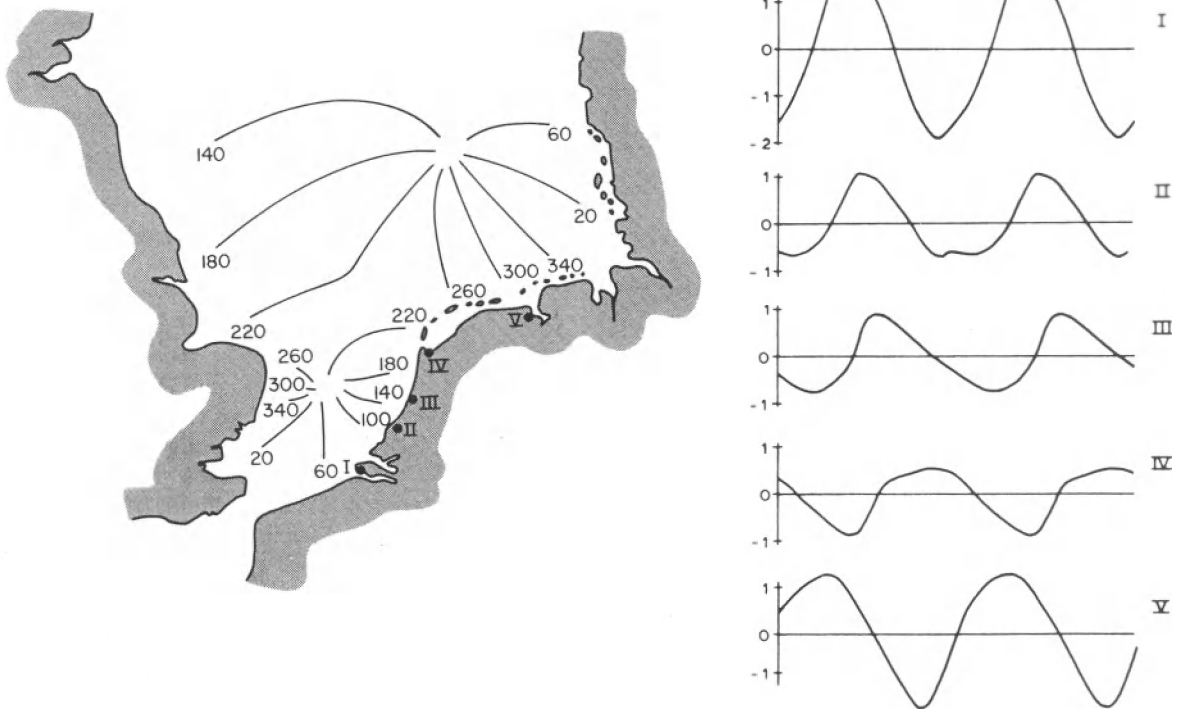


Fig. 3. Distortion of the tidal wave propagating along the Dutch coast (RIJKSWATERSTAAT).

sea boundary,  $l \ll L$ , the major part of the tidal wave is reflected at the head. The simplest schematization is a rectangular basin of constant depth. In the appendix the influence of the non-linear terms in the continuity equation and the momentum equation is demonstrated for such a simple geometry.

Without the friction term the tidal motion is almost a standing wave, slightly distorted by the non-linear terms  $d\xi u/dx$  and  $u du/dx$ . This distortion consists essentially of a relatively longer slack water period before ebb than before flood (Fig. 10d). The reason is that changes in water level propagate faster at high water than at low water; a nearly horizontal water surface is more readily reached and maintained. As a result the water level inclination and corresponding flow acceleration is larger in magnitude at low water than at high water.

The influence of the friction term is twofold. Firstly, part of the energy of the incoming tidal wave is absorbed; thus the reflected wave is smaller than the incoming wave: the tidal motion has the character of a partly progressive wave (IPPEN & HARLEMAN, 1966). Secondly, the frictional influence is less around high water than around low water. The effect is opposite to that of the other non-linear terms: around high water (just before and after slack water) the magnitude of the current is larger than around low water (see Fig. 10e)

$$|du/dt|_{SBE} > |du/dt|_{SBF}$$

In a tidal basin with landward decreasing depth the influence of friction is not the same when the tidal variation of the current velocity in a moving frame is considered. If the decrease in channel depth on the flood excursion of a fluid parcel exceeds the tidal range, then the friction experienced in the period around high water slack (SBE) is larger than the friction experienced around low water slack (SBF). Consequently,

$$|du/dt|_{SBF} > |du/dt|_{SBE}$$

for a fluid parcel moving with the tide: in a rectangular basin with landward decreasing depth, a landward residual transport of fine sediment is favoured.

The distortion of a tidal wave in basins of limited length due to both non-linear propagation terms and friction has been studied by several authors: KREISS (1957), HEATH (1981) and UNCLES (1981). They find that the maximum flood velocity exceeds the maximum ebb velocity, at least in the inner part of the estuary (in the absence of river discharge). The reason is again that water level changes propagate

faster around high water than around low water. The time delay between high water at different locations in the estuary is shorter than the delay between low water. Similarly the time delay between SBE at different locations is smaller than the time delay between SBF ( $dt^+/dx < dt^-/dx$ ). In other words, the flood duration in the inner part of the estuary is shorter than the ebb duration. Consequently, the maximum flood velocity exceeds the maximum ebb velocity. This effect is enhanced when frictional energy dissipation is important. In that case, water level variations are diffused through the estuary, rather than propagated. As shown by LE BLOND (1978), diffusion speed depends even more strongly on water depth than wave speed.

In the case of short tidal basins, distortion by non-linear terms is rather small. The water motion has essentially a co-oscillating character with nearly constant phase and water-level throughout the basin. In fact the most important causes for tidal asymmetry are (see also the studies of PETHICK, 1980; BOON & BYRNE, 1981):

- an asymmetry in the tidal boundary condition,
- a variation in the basin geometry with water-level.

In a co-oscillating tidal basin the current velocity can be obtained by integration of the continuity equation (1):

$$u = \frac{\Sigma}{A_s} \frac{\delta \xi}{\delta t} \Big|_{x=0} \quad (6)$$

Here  $\Sigma = \int_x^l b dx$  is the storage surface of the basin. This quantity, as well as the stream cross section  $A_s$ , depends on the water level  $\xi$ .

The influence of the tidal boundary condition  $\xi(t)$  on the current velocity follows directly from equation (6). As mentioned already, a distortion of the tidal wave propagating over the shallow coastal shelf influences the tidal motion in the adjacent estuaries. For example, the relatively fast rise and slow decrease of the tidal wave propagating along the Dutch coast is the major cause of the occurrence of a greater maximum current during flood than during ebb in the Dutch tidal basins (see Fig. 4). The boundary tide also affects the slack water periods before ebb and flood, but to a lesser degree. Here the major cause of asymmetry is the tidal variation of the basin geometry.

The time derivative at slack water of equation (6) yields:

$$\frac{du}{dt} \Big|_{\text{slack}} = \frac{\Sigma}{A_s} \frac{\delta^2 \xi}{\delta t^2} \Big|_{\text{slack}} \quad (7)$$

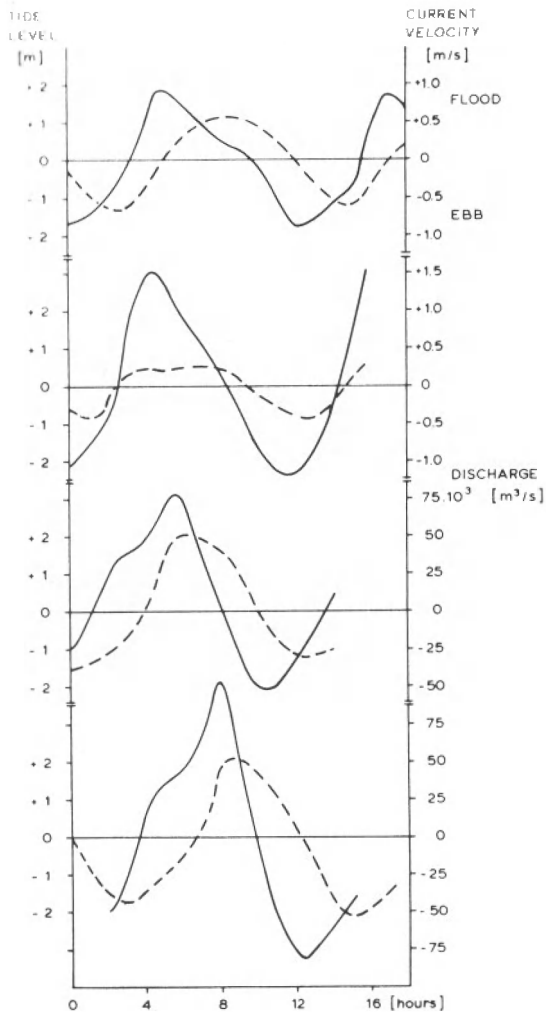


Fig. 4. Tidal variation of discharge/current velocity (—) and water level (---) in Dutch tidal basins (RIJKSWATERSTAAT, unpublished data).

On the basis of this expression one may distinguish between two types of tidal basins:

(1) The relative increase of stream cross-section  $A_s$  with increasing water-level is smaller than the relative increase of storage surface. The corresponding tidal basins have deep channels ( $h \gg a$ ) and/or high tidal flat areas (on the average above mean sea level). This characteristic favours a longer slack water period before flood than before ebb,  $|\dot{u}/\dot{t}|_{SBF} < |\dot{u}/\dot{t}|_{SBE}$ . Examples are shown in Fig. 5.

(2) The relative increase of stream cross-section with increasing water-level is greater than the relative increase of storage surface. The corresponding tidal basins have shallow channels (depth at most a few times larger than the tidal amplitude) and/or low tidal flat areas, which at high water become part of the

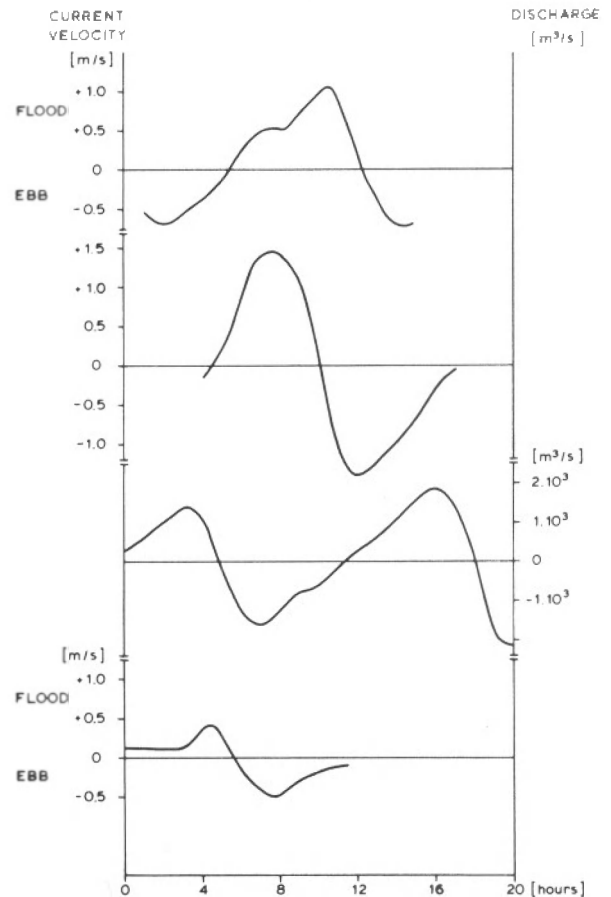


Fig. 5. Field observation of geometry-induced tidal wave deformation in type 1 tidal basins.

stream cross-section. This characteristic favours a longer slack water period before ebb,  $|\dot{u}/\dot{t}|_{SBE} < |\dot{u}/\dot{t}|_{SBF}$ . Examples are shown in Fig. 6.

The above implies that the tidal variation of the wetted geometry affects the residual transport of fine sediment. In the type 1 tidal basin, residual export of fine sediment is favoured. In the type 2 tidal basins, residual import of fine marine sediment can be expected and retention of the fine fluvial sediment discharged at the head.

It has been noted by SPEER & AUBREY (1985) and by BOON & BYRNE (1981) that large tidal flats may enhance the maximum ebb current. The tidal wave propagates faster in the channels than on the tidal flats. Therefore, the decrease in water-level during ebb takes place later on the tidal flat than in the channel. This leads to an important water-level inclination (see Fig. 1b) and a strong current during the last stage of the ebb period. A net seaward flux of coarse suspended sediment may result.

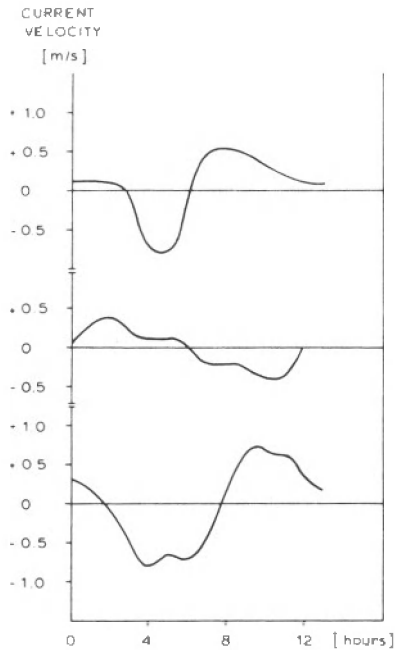


Fig. 6. Field observations of geometry-induced tidal wave deformation in type 2 tidal basins.

5. TIDAL ASYMMETRY AND SEDIMENT TRANSPORT IN THE WADDEN SEA AND THE EASTERN SCHELDT

In this section field observations in two tidal basins in the Netherlands will be discussed as an example of the more general principles established previously. In both tidal basins fresh water inflow is extremely small. The current distribution is mostly tide-induced; wind forcing is a secondary effect.

The morphology of the Wadden Sea Ameland area and the Eastern Scheldt basin is shown in Fig. 7, on the same scale. Both tidal basins are much shorter than the tidal wave length. In the Eastern Scheldt large deep channels bounded by levees lead to tidal flats situated in the landward part; in the Wadden Sea a sequence of large, medium and small channels rapidly lead from deep to shallow regions. According to these morphological differences the tidal wave is distorted differently in both systems. This is most pronounced for the slack water periods. In Fig. 8 the bathymetry of the two tidal basins is represented by the curves showing the surface at different depths. In the Wadden Sea the relative increase of the volume with

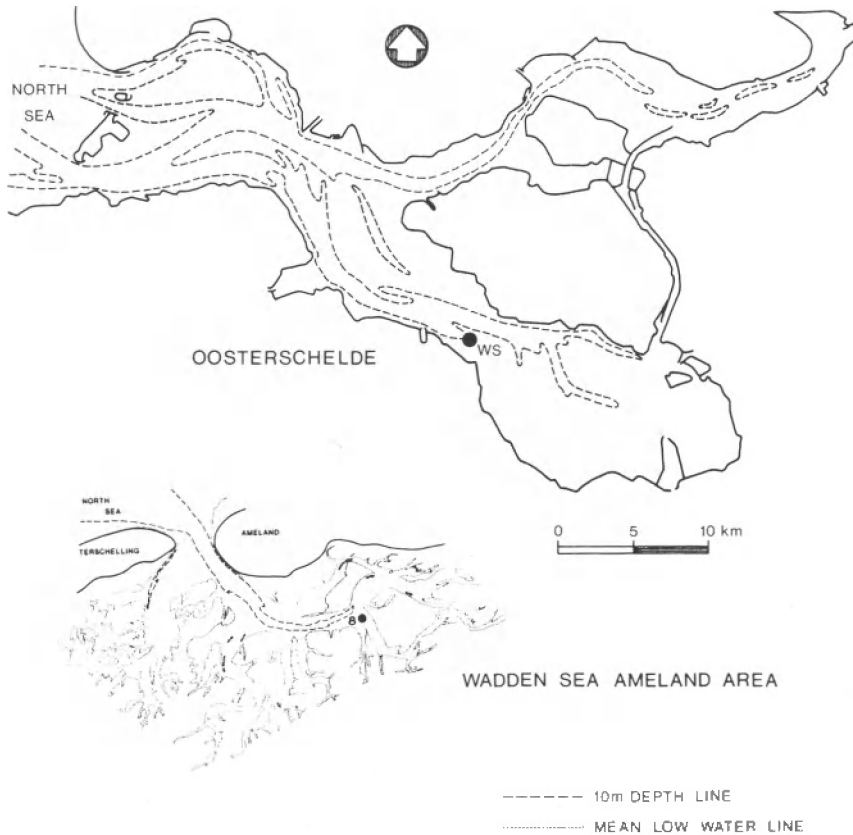
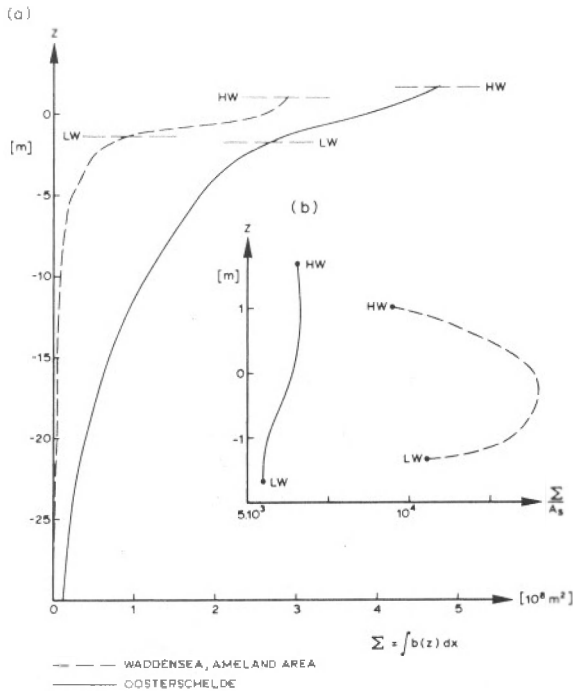


Fig. 7. Morphology of the Wadden Sea Ameland area and the Eastern Scheldt basin.



BATHYMETRY OF OOSTERSCHELDE AND AMELAND TIDAL SYSTEMS:  
(a) SURFACE AS A FUNCTION OF DEPTH  
(b) RATIO OF STORAGE AREA  $\Sigma$  AND STREAM CROSS-SECTION  $A_s$   
AS A FUNCTION OF TIDAL LEVEL

Fig. 8. Surface as a function of depth in the Wadden Sea Ameland area and the Eastern Scheldt basin; the ratio  $\Sigma/A_s$  as a function of tidal level.

tidal level is greater than the relative increase of surface. The ratio  $\Sigma/A_s$  at high water is smaller than at low water. According to equation (7) one may expect, in the Wadden Sea  $|du/dt|_{SBE} < |du/dt|_{SBF}$ . In the Eastern Scheldt the opposite inequality should hold. Fig. 9 shows the agreement of these predictions with field data.

The peak flood discharge slightly exceeds the peak ebb discharge in both the Wadden Sea and the Eastern Scheldt for an average tide, see Fig. 4. The extent of tidal flat areas is insufficient to cancel the flood dominance due to the faster rise and slower decrease of the tide along the Dutch coast (see Fig. 3). (Locally ebb currents may dominate flood currents due to the presence of ebb and flood dominated channels). Therefore, flood transport of coarse sediment should in principle exceed ebb transport.

The tidal boundary curves (Fig. 3) further show that the second derivative  $\partial^2 \xi / \partial t^2$  presents a different asymmetry in the Wadden Sea and in the Eastern Scheldt. In the Wadden Sea  $|\partial^2 \xi / \partial t^2|_{HW} < |\partial^2 \xi / \partial t^2|_{LW}$ . This means that the distortion of the tidal wave running along the Dutch coast also contri-

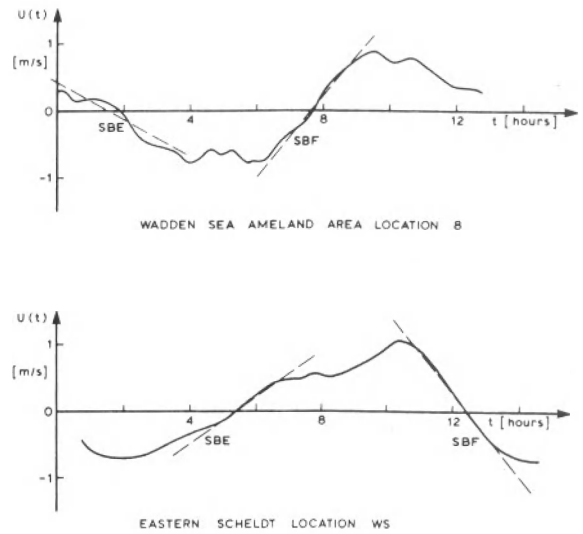


Fig. 9. Current velocity variation in the Wadden Sea Ameland area (location 8) and in the Eastern Scheldt basin (location WS).

butes to the inequality  $|du/dt|_{SBE} < |du/dt|_{SBF}$ . In the Eastern Scheldt the boundary tide contributes to the opposite inequality.

Large tidal flats are present in the Wadden Sea and in the Eastern Scheldt. The major part is covered only around high water. In this period bottom material (fine and coarse sediment) can be brought in suspension and subsequently be transported by ebb currents. Thus the residual landward transport by tidal currents of both coarse and fine sediment is counteracted. In the Wadden Sea the fine sediment fraction in the intertidal areas is much larger than in the Eastern Scheldt. Therefore, one may expect that the influence of wind waves affects more strongly the fine sediment transport in the Wadden Sea.

One may also expect that a residual landward transport of sediment prevails under calm weather conditions, while seaward transport dominates under storm conditions.

Field observations show the following: In the Wadden Sea, bottom soundings over a period of 20 years indicate an average bottom accretion of  $0.5-1 \text{ cm} \cdot \text{a}^{-1}$  (DE BOER & VISSER, 1981). In the Eastern Scheldt, over the period 1872-1974 an average erosion of  $1 \text{ cm} \cdot \text{a}^{-1}$  is found, VAN DEN BERG (1984). However, the net erosion rate has decreased in the last decade and does not exceed a few  $\text{mm} \cdot \text{a}^{-1}$ . An extensive sediment transport measurement campaign covering a whole year, but excluding storm periods yielded a net export of sediment (essentially fine sediment) corresponding to an average erosion of 0 to  $3 \text{ cm} \cdot \text{a}^{-1}$  (DRONKERS, 1985).

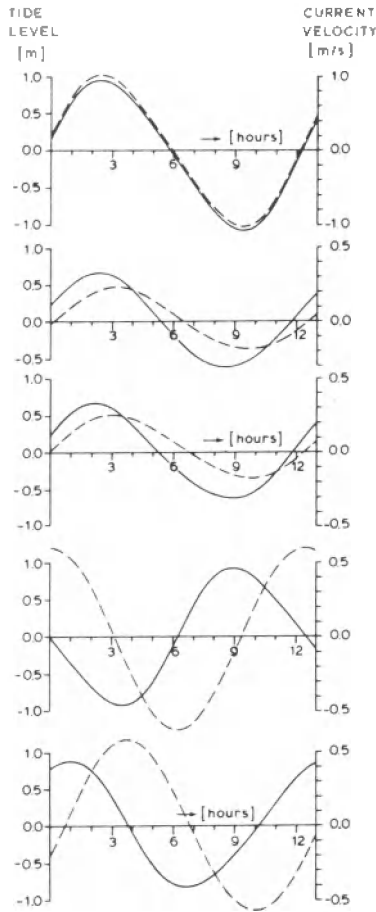


Fig. 10. Time variation of water-level (---) and current velocity (—) in a uniform channel with open sea boundary.  $\xi = a \cos \omega t$  at  $x=0$ . The amplitude  $a=1$  m, the depth  $h=10$  m; for damped waves the friction coefficient  $F=0.002 \text{ m s}^{-1} \cdot a$ . a. Progressive non-linear wave without friction at  $x=100$  km. b. Progressive damped wave, without non-linear terms  $\partial u \xi / \partial u$ ,  $u \partial u / \partial x$ . c. Progressive damped non-linear wave. d. Standing non-linear wave without friction at  $x=25$  km in a canal of length  $l=50$  km. e. Standing damped wave, without non-linear terms  $\partial u \xi / \partial x$ ,  $u \partial u / \partial x$ .

The expression (1) for tide-induced residual transport of fine sediment yields a net import corresponding to an average bottom accretion of  $1.6 \text{ cm} \cdot \text{a}^{-1}$  for the Wadden Sea, and for the Eastern Scheldt a net export corresponding to an average bottom erosion of  $0$  to  $0.5 \text{ mm} \cdot \text{a}^{-1}$ .

A comparison of the field observations with the predictions for fine sediment transport, taking into account the qualitative tendencies that have been indicated for storm affects and for the residual transport of coarse sediment, allows the conclusion that:

- for fine sediment, the observed and predicted di-

rections of the residual fluxes are in agreement.

- the magnitude of the residual flux of fine sediment is strongly influenced by wind waves, and storms, especially in the Wadden Sea (see also WINKELMOLEN & VEENSTRA, 1980; DRONKERS, 1985)

- for coarse suspended sediment the landward direction of the tide-induced residual flux in the Wadden Sea agrees with observations. In the Eastern Scheldt an important contribution to the residual transport of coarse suspended sediment seems to be provided by the action of wind waves in combination with tidal transport. The stronger impact of wind waves in the Eastern Scheldt compared to the Wadden Sea can also be traced to the different orientations of these basins with respect to the average wind direction: in the Eastern Scheldt the direction of the main channel axis fits the average wind direction more closely.

The field observations indicate that a morphological equilibrium in the Wadden Sea and the Eastern Scheldt is not yet reached in the period under consideration. However, different processes involving wind- and tide-induced processes yield mutually counteracting residual fluxes of the same order of magnitude. This implies that small morphological changes can alter the total residual transport: the actual state cannot be very far from morphological equilibrium. In fact, the major external change in the Wadden Sea Ameland area during the past decades is an increase of the mean sea level of  $0.2 \text{ cm} \cdot \text{a}^{-1}$  on the average. If the sea level stabilizes, the most probable evolution of the Wadden Sea is a further accretion of the tidal flats until a quasi-equilibrium between tide- and wind-induced sediment fluxes is reached.

In the Rhine-Meuse-Scheldt delta successive engineering works have caused a considerable increase of the tidal prism in the Eastern Scheldt during the period 1872-1974 and in particular between 1965 and 1970. The tidal energy dissipation in the Eastern Scheldt increased. Erosion dominated over sedimentation and ebb sediment fluxes over flood sediment fluxes, especially in periods shortly after man-induced alterations of the hydraulic regime. In the future a storm surge barrier in the mouth of the Eastern Scheldt, presently under construction, will decrease again the tidal influence and the sediment motion in this basin. A slow infill with sediment is expected.

## 6. SUMMARY AND CONCLUSIONS

1) The most pertinent features of tidal wave distortion for residual sediment transport are:

- a difference between the slack water periods before ebb and flood ( $|du/dt|_{\text{SBE}} \neq |du/dt|_{\text{SBF}}$ ),

which affects in particular the residual transport of the fine fraction of the suspended load.

- a difference between the maximum currents during ebb and flood ( $u_{\text{ebb}}^{\text{max}} \neq u_{\text{flood}}^{\text{max}}$ ), which especially affects the residual transport of the coarse fraction of the suspended load.

2) In regularly shaped basins (no important width variation with water-level) and in the absence of river inflow, the tidal wave tends to be distorted such that  $u_{\text{flood}}^{\text{max}} > u_{\text{ebb}}^{\text{max}}$ ,  $|du/dt|_{\text{SBE}} < |du/dt|_{\text{SBF}}$ . This distortion is manifest in the inner part of both long and short tidal basins (compared to the tidal wave length). It will cause a sediment infill of estuaries in periods of small river discharge.

3) In irregularly shaped estuaries (meandering and braiding channel system, tidal flats) the tidal current variation is influenced by the geometry. Two types of geometry can be distinguished:

- shallow channels/landward decreasing depth, tidal flats below mean sea level.

- deep channels throughout, tidal flats above mean sea level.

In the first case the slack water period before ebb will exceed the slack water period before flood: a residual import of fine sediment is favoured. In the second case the inverse situation occurs.

In addition, large tidal flats cause an enhancement of the maximum ebb current and may, therefore, induce a seaward flux of coarse suspended sediment.

4) The distortion of the tidal wave propagating on the coastal shelf also induces an ebb-flood asymmetry in the tidal current variation inside adjacent bays and estuaries. If the rise of the coastal water-level is faster than the decrease, in a co-oscillating tidal basin  $u_{\text{flood}}^{\text{max}} > u_{\text{ebb}}^{\text{max}}$  and a sediment infill is favoured.

5) Wind induced resuspension of sediment may also present a tidal asymmetry. In many estuaries the major part of the fine grained tidal flats are covered around high water only. In such cases wind induced resuspension leads to an export of fine sediment.

## 6. REFERENCES

- AIRY, G.B., 1842. Tides and waves. *Encycl. Metrop.*, London.
- ALLEN, G.P., G. SAUZAY, P. CASTAING & J.M. JOUANNEAU, 1977. Transport and deposition of suspended sediment in the Gironde estuary, France. In: M. WILEY. *Estuarine processes* Vol. 2. Academic Press N.Y.: 63-81.
- ANDERSON, F.E., 1972. Resuspension of estuarine sediments by small amplitude waves—*J. sedim. Petrol.* **42**: 602-607.
- ARIATHURAI, R., R.E. MACARTHUR & R.B. KRONE, 1977. Mathematical model of estuarial sediment transport. Tech. Rep. D-77-12, Environmental Effects Laboratory, U.S. Army Engineers Waterways Experiment Station: 1-70.
- AVOINE, J., G.P. ALLEN, M. NICHOLS, J.C. SALOMON & C. LARSONNEUR, 1981. Suspended-sediment transport in the Seine estuary, France: effect of man-made modifications on estuary-shelf sedimentology—*Mar. Geol.* **40**: 119-137.
- BERG VAN DEN, J.R., 1984. Morphological changes of the ebb-tidal delta of the Oosterschelde during recent decades—*Geologie Mijnb.* **63**: 363-375.
- BIGGS, R.B., 1978. Coastal bays. In: R.A. DAVIS. *Coastal sedimentary environments*. Springer Verlag: 1-420.
- BOER, M. DE & G.C. VISSER, 1981. *Erosie en sedimentatie in de westelijke Waddenzee*. Nota WVKZ- 80.H001, Rijkswaterstaat, The Netherlands: 1-38.
- BOON, J.D. & R.J. BYRNE, 1981. On basin hypsometry and the morphodynamic response of coastal inlet systems—*Mar. Geol.* **40**: 27-48.
- BRUUN, P., 1978. *Stability of tidal inlets*. Elsevier Amsterdam: 1-510.
- CHASE, R.R.P., 1979. Settling behavior of natural aquatic particulates—*Limnol. Oceanogr.* **24**: 417-426.
- COMOY, M., 1881. *Étude pratique sur les marées fluviales et la mascaret*. Paris.
- CREUTZBERG, F. & H. POSTMA, 1979. An experimental approach to the distribution of mud in the southern North Sea—*Neth. J. Sea Res.* **13**: 99-116.
- DANKERS, N., M. BINSBERGEN, K. ZEGERS, R. LAANE & M. RUTGERS VAN DER LOEFF, 1984. Transportation of water, particulate and dissolved organic and inorganic matter between a salt marsh and the Ems-Dollard estuary, the Netherlands—*Estuar. coast. Shelf Sci.* **19**: 143-165.
- DRONKERS, J., 1985. Tide-induced residual transport of fine sediment. In: J. VAN DE KREEKE. *Proceedings of the Symposium on the physics of shallow bays and estuaries*, Miami 1984. Springer Verlag (in press).
- DYER, K.R., 1980. Velocity profiles over a rippled bed and the threshold of movement of sand—*Estuar. coast. mar. Sci.* **10**: 181-199.
- EINSTEIN, H.A. & R.B. KRONE, 1962. Experiments to determine modes of cohesive transport in salt water—*J. geophys. Res.* **67**: 1451-1461.
- EISMA, D., J. KALF & M. VEENHUIS, 1980. The formation of small particles and aggregates in the Rhine estuary—*Neth. J. Sea Res.* **14**: 172-191.
- FESTA, J.P. & D.V. HANSEN, 1978. Turbidity maxima in partially mixed estuaries: a two-dimensional numerical model—*Estuar. coast. mar. Sci.* **7**: 347-359.
- GODIN, G., 1985. Modification of river tides by the discharge—*J. WatWay port coast. ocean Engng* **111**: 257-274.
- HANSEN, W., 1962. Tides. In: M.N. HILL. *The Sea*, Vol. I. John Wiley N.Y.: 764-801.
- HARLEMAN, D.R.F., 1971. One-dimensional models. In: *Estuarine modelling: an assessment*. Tracor Inc., Austin, Texas: 50-51.
- HEATH, R.A., 1980. Phase relations between the over- and fundamental-tides—*Dt. hydrogr. Z.* **33**: 177-191.
- HEATHERSHAW, A.D., 1981. Comparisons of measured and predicted sediment transport rates in tidal currents—*Mar. Geol.* **42**: 75-104.
- HEATHERSHAW, A.D. & D.C. HAMMOND, 1980. Secondary circulations near sand banks and in coastal embayments—*Dt. hydrogr. Z.* **33**: 135-151.

- INGLIS, C.C. & F.H. ALLEN, 1957. The regimen of the Thames estuary as affected by currents, salinity and river flow.—*Proc. Inst. civ. Engng* **7**: 827-868.
- IPPEN, A.T. & D.R.F. HARLEMAN, 1966. Tidal dynamics in estuaries. In: A.T. IPPEN. *Estuary and coastline hydrodynamics*. McGraw-Hill, 493-545.
- IWAGAKI, Y. & T. SAKAI, 1972. Shoaling of finite amplitude long waves on a beach of constant slope.—*Proc. Conf. coast. Engng* **13** (1): 347-364.
- KJERFVE, B., L.H. STEVENSON, J.A. PROEHL, T.H. CHRZANOWSKI & W.M. KITCHENS, 1981. Estimation of material fluxes in an estuarine cross section: a critical analysis of spatial measurement density and errors.—*Limnol. Oceanogr.* **26**: 325-335.
- KREISS, H., 1957. Some remarks about non-linear oscillations in tidal channels.—*Tellus* **9**: 53-68.
- LAMB, H., 1932. *Hydrodynamics*. Cambridge Univ. Press: 1-738.
- LAMBIASE, J.L., 1980. Hydraulic control of grain-size distributions in a macrotidal estuary.—*Sedimentology* **27**: 433-446.
- LE BLOND, P.H., 1978. On tidal propagation in shallow rivers.—*J. geophys. Res.* **83** (C9): 4717-4721.
- LYNCH, D.K., 1982. Tidal bores.—*Scient. Am.* **247**: 134-143.
- MCDOWELL, D.M. & B.A. O'CONNOR, 1977. Hydraulic behaviour of estuaries. *Civil engng hydraul. Series*, MacMillan, London: 1-292.
- MEADE, R.H., 1972. Transport and deposition of sediments in estuaries.—*Mem. geol. Soc. Am.* **133**: 91-120.
- MEHTA, J.A. & E. PARTHENIADES, 1982. Resuspension of deposited cohesive sediment bed.—*Proc. Conf. coast. Engng* **18** (2): 1569-1588.
- MIGNIOT, C., 1968. Études des propriétés physiques de différents sédiments très fins et de leur comportement sous des actions hydrodynamiques.—*Houille Blanche* **7**: 591-620.
- ODD, N.C.M. & N.W. OWEN, 1972. A two layer model of mud transport in the Thames estuary. *Proc. Inst. civ. Engng, Suppl.* 1972 (9), paper 7517S: 175-205.
- PETHICK, J.S., 1980. Velocity surges and asymmetry in tidal channels.—*Estuar. coast. mar. Sci.* **11**: 331-345.
- PINGREE, R.O., D.K. GRIFFITHS & L. MADDOCK, 1984. Quarter diurnal shelf resonances and tidal bed stress in the English Channel.—*Contin. Shelf Res.* **3**: 267-289.
- POSTMA, H., 1960. Einige Bemerkungen über den Sinkstofftransport im Ems-Dollart Gebiet.—*Verh. K. ned. geol. mijnb. Genoot. (Geol. Ser.)* **19**: 103-110.
- , 1961. Transport and accumulation of suspended matter in the Dutch Wadden Sea.—*Neth. J. Sea Res.* **1**: 148-190.
- , 1967. Sediment transport and sedimentation in the marine environment. In: G.H. LAUFF. *Estuaries, Am. Ass. Adv. Sci.*, Washington: 158-179.
- , 1980. Sediment transport and sedimentation. In: E. OLAUSSON & I. CATO. *Chemistry and biogeochemistry of estuaries*. John Wiley, Chichester: 153-186.
- RIJKSWATERSTAAT. Tide tables for the Netherlands. Staatsuitgeverij, The Hague.
- ROBINSON, A.H.W., 1960. Ebb-flood channel systems in sandy bays and estuaries.—*Geography* **45**: 183-199.
- SCHUBEL, J.R. & R.H. MEADE, 1977. Man's impact on estuarine sedimentation. *Proc. Conf. est. poll. Control and Assess, Vol. 1*. US env. Prot. Agency, Washington: 193-209.
- SPEER, P.E. & D.G. AUBREY, 1985. A study of non-linear tidal propagation in shallow inlet/estuarine systems, part II Theory.—*Estuar. coast. Shelf Sci.* **21**: 207-224.
- STRAATEN, L.M.J.U. VAN & P.H. KUENEN, 1957. Accumulation of fine-grained sediments in the Dutch Wadden Sea.—*Geologie Mijnb. (N.S.)* **19**: 329-354.
- UNCLES, R.J., 1981. A note on tidal asymmetry in the Severn estuary.—*Estuar. coast. mar. Sci.* **13**: 419-432.
- UNCLES, R.J., R.C.A. ELLIOT & S.A. WESTON, 1985. Observed fluxes of water, salt and suspended sediment in a partly mixed estuary.—*Estuar. coast. Shelf Sci.* **20**: 147-167.
- VEEN, J. VAN, 1950. Eb- en vloed-scharen in de nederlandse getijwateren.—*Tijdschr. K. ned. aardrijksk. Genoot.* **67**: 303-335.
- WINKELMOLEN, A.H. & H.J. VEENSTRA, 1980. The effect of a storm surge on nearshore sediments in the Ameland-Schiermonnikoog area.—*Geologie Mijnb.* **59**: 97-111.
- WALLIS, S.G. & D.W. KNIGHT, 1984. Calibration studies concerning a one-dimensional numerical tidal model with particular reference to resistance coefficients.—*Estuar. coast. Shelf Sci.* **19**: 541-562.
- YALIN, M.W., 1972. *Mechanics of sediment transport*. Pergamon Press, Oxford: 1-290.

## APPENDIX

The one-dimensional tidal equations (1-2) are solved for uniform systems (constant depth, width) to first order in  $a/h$ , according to standard methods as indicated, e.g. in LAMB (1932). For distinction between the impacts of the different non-linear terms, multiplication factors  $f_1$ ,  $f_2$  and  $f_3$  have been introduced. The equations read

$$\frac{d\xi}{dt} + h \frac{du}{dx} + f_1 \frac{d\xi u}{dx} = 0 \quad (\text{A1})$$

$$\frac{du}{dt} + f_2 u \frac{du}{dx} + g \frac{d\xi}{dx} + F \frac{u}{h} - f_3 F \frac{u\xi}{h} = 0 \quad (\text{A2})$$

Solutions are presented for systems with a prescribed water-level variation at the ocean boundary:  $\xi(t) = a \cos \sigma t$ . The solutions presented in HEATH (1980) for the same tidal equations (but with a quadratic friction law) satisfy different boundary conditions. The qualitative features of the solutions appear to be similar, however.

## SOLUTIONS FOR PROGRESSIVE WAVES

1. Without friction ( $F=0$ ), see Fig. 10a.

$$\xi = a \left[ \cos(\sigma t - kx) - (f_1 + 2f_2) \frac{1}{4} \frac{a}{h} kx \sin(2\sigma t - 2kx) \right]$$

$$u = \frac{\sigma a}{kh} \left[ \cos(\sigma t - kx) - \frac{a}{h} \left( \frac{1}{2} + \frac{1}{8} (2f_2 - f_1) \cos(2\sigma t - 2kx) + \frac{1}{4} (2f_2 + f_1) kx \sin(2\sigma t - 2kx) \right) \right]$$

Here the wave number  $k$  is given by  $k = \sigma / \sqrt{gh}$ . The validity of these solutions is restricted to

$$x \ll h/ka$$

(LAMB, 1932)

2. Non-linear friction ( $F > 0$ ,  $f_3 = 1$ ) but no other non-linear terms ( $f_1 = f_2 = 0$ ), see Fig. 10b.

$$\xi = \frac{a^2}{2h} \frac{k_R^2}{|k|^2} (1 - e^{2k_I x}) + \frac{1}{2} a \left[ e^{i(\sigma t - kx)} - \frac{a}{2h} \left( e^{2i(\sigma t - kx)} - e^{2i(\sigma t - k'x)} \right) + \text{c.c.} \right]$$

$$u = \frac{\sigma a}{2h} \left[ \frac{1}{k} e^{i(\sigma t - kx)} - \frac{a}{2h} \left( \frac{1}{k} e^{2i(\sigma t - kx)} - \frac{1}{k'} e^{2i(\sigma t - k'x)} \right) + \text{c.c.} \right]$$

Here  $k$  and  $k'$  are complex wave numbers,  $k_R = \text{Re } k > 0$ ,  $k_I = \text{Im } k < 0$ ,

$$k^2 = \frac{\sigma(\sigma - j \frac{F}{h})}{gh}, \quad k'^2 = \frac{\sigma(\sigma - j \frac{F}{2h})}{gh}$$

3. Non-linear friction ( $F > 0$ ,  $f_3 = 1$ ) and non-linear terms ( $f_1 = f_2 = 1$ ), see Fig. 10c.

$$\xi = B(1 - e^{2k_I x}) + \frac{1}{2} a \left[ e^{i(\sigma t - kx)} + A \left( e^{2i(\sigma t - kx)} - e^{2i(\sigma t - k'x)} \right) + \text{c.c.} \right]$$

$$u = C e^{2k_I x} + \frac{\sigma a}{2h} \left[ \frac{1}{k} e^{i(\sigma t - kx)} + \left( A - \frac{a^2}{4h^2} \right) \frac{1}{k} e^{2i(\sigma t - kx)} - \frac{A}{k'} e^{2i(\sigma t - k'x)} \right] + \text{c.c.} \right]$$

$$\text{Here } A = -\frac{a}{2F} \left( 2 \frac{F}{h} + 3i\sigma \right), \quad B = \frac{\sigma^2 a^2}{4gh^2 |k|^2} \left( 1 - 2 \frac{F}{h\sigma} \frac{k_R}{k_I} \right), \quad C = -\frac{\sigma a^2 k_R}{2h^2 |k|^2}$$

## SOLUTIONS FOR STANDING WAVES

A basin is considered with a closed end at  $x=l$  and an ocean boundary at  $x=0$ .

4. Non-linear terms ( $f_1, f_2 \neq 0$ ), no friction ( $F=0$ ), see Fig. 10d.

$$\xi = \frac{a}{\cos kl} \left[ \cos k(l-x) \cos \omega t - (f_1 + 2f_2) \frac{1}{8} \frac{a^2}{h^2} kx \cos 2k(l-x) \cos 2\omega t \right]$$

$$u = -\frac{\omega a}{kh \cos kl} \left[ \sin k(l-x) \sin \omega t - \frac{a}{h} \left( \frac{1}{16} (2f_2 - f_1) + \frac{1}{8} (2f_2 + f_1) k \left[ 1 + (l-x) \cot 2k(l-x) \right] \right) \sin 2k(l-x) \sin 2\omega t \right]$$

5. Non-linear friction ( $F > 0, f_3 = 1$ ), no other non-linear terms ( $f_1 = f_2 = 0$ ), see Fig. 10e.

$$\xi = \frac{F \omega a^2}{4g h^3 |k|^2} \frac{k^2 l \left[ \cos 2k_R l - \cos 2k_R(l-x) \right] + k^2 l \left[ \cosh 2k_I l - \cosh 2k_I(l-x) \right]}{k_R k_I \left[ \cos 2k_R l + \cosh 2k_I l \right]}$$

$$+ \frac{1}{2} a \left[ \frac{\cos k(l-x)}{\cos kl} e^{i\omega t} - \frac{a}{4h \cos^2 kl} \left( \cos 2k(l-x) - \frac{\cos 2kl}{\cos 2k'l} \cos 2k'(l-x) \right) e^{2i\omega t} + c.c. \right]$$

$$u = i \frac{\omega a}{2h} \left[ \frac{\sin k(l-x)}{k \cos kl} e^{i\omega t} - \frac{a}{4h \cos^2 kl} \left( \frac{\sin 2k(l-x)}{k} - \frac{\cos 2kl}{\cos 2k'l} \frac{\sin 2k'(l-x)}{k'} \right) e^{2i\omega t} + c.c. \right]$$